Performance of Adaptive Volterra Equalizers on Nonlinear Satellite Channels

Alberto Gutierrez and William E. Ryan
Center For Space Telemetering and Telecommunications Systems
New Mexico State University
Las Cruces, NM 88003-0001

ABSTRACT— Adaptive nonlinear Volterra equalizers are developed for compensation of nonlinear signal distortion in a satellite communications channel. The equalizers do not require a Volterra characterization of the channel and adaption of the weights is accomplished with the least-mean square (LMS) algorithm. Convergence of the equalizers are discussed as well as a multiple-step LMS adaption method which improves the convergence characteristics. We compare the performance and complexity of these equalizers to that of a linear equalizer for QPSK, 8-PSK and 16-QAM.

I. Introduction

Satellite communication channels must employ a high power amplifier (HPA) in order to provide sufficient link margin. The increasing demand for bandwidth and the desire to minimize satellite power consumption often means the HPA is driven at or near saturation. The end result is the introduction of nonlinear bandlimited signal distortion yielding nonlinear intersymbol interference (ISI). For such systems, it may be useful to compensate for this nonlinear ISI.

One possibility for nonlinear signal compensation is in the form of an adaptive nonlinear Volterra equalizer. The use of nonlinear equalization is not new. Nonlinear equalization of voice channels was studied in [1]. Nonlinear equalization of digital satellite channels using Volterra kernels was studied for satellite communication systems by Benedetto and Biglieri [2]. However, [2] limits its analysis to signal distortion caused by the nonlinear bandlimited system, it does not take into account noise, and it is not adaptive. An extensive analysis of a satellite communication system using Volterra Series is presented in [3] including noise but not including equalization. Volterra equalization was also analyzed and compared to other signal compensation approaches such as predistortion, and ISI cancellation in [4] for microwave radio channels employing M-QAM modulation.

The systems studied in [4] were for QAM with modulation levels of 64, 128, and 256. Since these systems have a constellation with signal points which are not on a constant modulus, they are highly sensitive to the AM/AM and AM/PM distortion caused by the HPA. Also, the modulation orders studied required a high signal to noise ratio for reasonable error rates. In this work we consider M-PSK systems which employ a constellation with signal points on a constant modulus and operate at lower signal to noise ratios. We also consider 16-QAM whose signal points are not on a constant modulus, but operates at lower signal to noise ratios than the systems in [4]. The present work adds adaption to the Volterra equalizer and presents several examples of digital satellite communication channel performance utilizing adaptive Volterra equalizers. We use as our performance criteria both mean-square error (MSE) and bit error probability (P_b).

The following section introduces the channel model and description of the Volterra equalizer. Section III describes the adaption algorithm, convergence issues, and suggests a multiple-step adaption algorithm for increasing the rate of convergence while maintaining stability. Section IV presents several results obtained from computer simulations followed by the conclusions in Section V.

II. Channel and Equalizer Models

The block diagram of a satellite communications channel with downlink noise is shown in Fig. 1. The modulated input to the satellite, x(t), is filtered by the channel pre-filter then amplified by an HPA, a traveling wave tube (TWT). The output of the TWT is filtered by the channel post filter and summed with additive white Gaussian yielding r(t). The signal r(t) is then filtered by the receive filter to yield the output of the system, y(t).

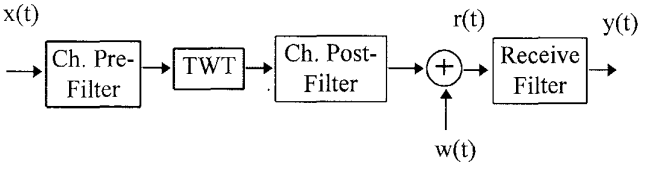

Figure 1. Satellite Communication Channel

The TWT is modeled, following Saleh [5], as a frequency-independent memoryless bandpass nonlinearity. It is completely characterized by its AM/AM and AM/PM conversions, respectively, given by

$$A(r) = \alpha_a / (1+\beta_a r^2), \qquad \text{(AM/AM)} \qquad (1)$$

and,

$$\Phi(r) = \alpha_\phi r^2 / (1+\beta_\phi r^2), \qquad \text{(AM/PM)} \qquad (2)$$

where r is the amplitude of the input waveform, $\alpha_q = 1.9638$, $\beta_a = 0.9945$, $\alpha_\phi = 2.5293$, and $\beta_\phi = 2.8168$. If r(t) and $\theta(t)$ are the instantaneous input modulus and phase, respectively, of the TWT then A(r(t)) and $\Phi(r(t))+\theta(t)$ represent the instantaneous amplitude and phase, respectively, of the TWT output. Because

This work supported by NASA grants NAG 5-1491 and NGT-50898

the TWT is between two linear filters the overall channel is a nonlinear system with memory. The effects of the nonlinear bandlimited channel on the signaling waveform include a distortion of the HPA output spectrum and nonlinear ISI [6].

The Volterra series characterization of a nonlinear communication channel provides a relationship between the discrete-time input symbols, X_n, and the discrete-time channel output symbols, $Y_n=y(nT_s)$ where T_s is $1/R_s$ (R_s = symbol rate), and is given [2,3] by

$$Y_n = \sum_{n_1} C_{n_1} X_{n-n_1} + \sum_{n_1}\sum_{n_2}\sum_{n_3} C_{n_1 n_2 n_3} X_{n-n_1} X_{n-n_2} X^*_{n-n_3} + \sum_{n_1}\sum_{n_2}\sum_{n_3}\sum_{n_4}\sum_{n_5} C_{n_1 n_2 n_3 n_4 n_5} X_{n-n_1} X_{n-n_2} X_{n-n_3} X^*_{n-n_4} X^*_{n-n_5} + \cdots \quad (3)$$

This equation represents a low-pass equivalent discrete-time channel model. As indicated in (3), Y_n consists of linear and nonlinear ISI (intersymbol interference) terms. The C_{n_1}, $C_{n_1}C_{n_2}C_{n_3}$, ... are constant coefficients determined from the Volterra characterization of the channel [2,3]. The X_{n-n_i} (i=1,2, ...) are the channel inputs for time $n-n_i$, and * denotes complex conjugation. Notice that the nonlinear terms consist of odd degree multiples of the discrete-time channel inputs. This is because nonlinear combinations of even degree are assumed to be out of the band of interest.

Equation (3) suggests the form of the nonlinear Volterra equalizer with inputs Y_n. The output of the equalizer, Z_n, consists of a linear combination of all linear terms and all possible combinations of nonlinear terms of Y_n, of odd degree, and is given by

$$Z_n = \sum_{n_1} w_{n_1} Y_{n-n_1} + \sum_{n_1}\sum_{n_2}\sum_{n_3} w_{n_1 n_2 n_3} Y_{n-n_1} Y_{n-n_2} Y^*_{n-n_3} + \sum_{n_1}\sum_{n_2}\sum_{n_3}\sum_{n_4}\sum_{n_5} w_{n_1 n_2 n_3 n_4 n_5} Y_{n-n_1} Y_{n-n_2} Y_{n-n_3} Y^*_{n-n_4} Y^*_{n-n_5} + \cdots \quad (4)$$

In practice, any channel has a finite memory and nonlinearity of finite degree, so that the summations in (3) and (4) are finite.

Fig. 2 illustrates a block diagram of a 3-tap 3rd-order Volterra equalizer, where Y_0 in the figure corresponds to the Y_n in (4). The samples from a tapped delay line are the inputs to a nonlinear combiner. The nonlinear combiner then outputs all single taps and all combinations of three taps. Each output from the nonlinear combiner is then scaled by a weight to form an input to the summing device. In general there are

$$L = \sum_{i=1}^{(order+1)/2} N^{2i-1} \quad (5)$$

terms out of the nonlinear combiner, where N is the number of taps in the tapped delay line, "order" is highest degree term at the nonlinear combiner output, and is restricted to odd numbers. Thus, from (5), the equalizer in Fig. 2 contains 30 outputs from

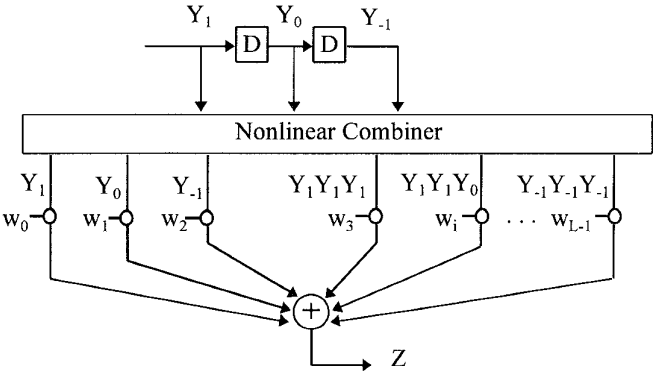

Figure 2. 3-tap 3rd-order Volterra equalizer.

the nonlinear combiner, 3 linear and 27 of degree 3. It is also possible to have a nonlinear equalizer with N-tap linear compensation, but with a subset of the taps forming nonlinear combinations. Performance of equalizers of this form are presented in the simulation results section.

In [2], a significant reduction in complexity is made, for M-PSK systems, by eliminating terms from the nonlinear combiner of the form $Y_iY_jY_k^* = Y_j$ for i or j = k, assuming Y_n is of modulus one. Because Y_n contains a noise term, this reduced complexity equalizer suffers a performance degradation as is demonstrated in the simulation results section.

III. Volterra Equalizer Adaption and Convergence

Since the nonlinear combining occurs before the tap weights of the equalizer, the outputs of the nonlinear combiner may be considered inputs to a linear adaptive filter. Thus, the LMS algorithm, [7] may be employed for adaption and the results of linear filtering apply. However, obtaining a correlation matrix for the outputs of the nonlinear combiner may be difficult.

Denote the output of the nonlinear combiner by the complex vector $\mathbf{U} = [u_0\ u_1 \cdots u_{L-1}]^T$ where T denotes transpose, the number of elements, L, in the vector is given by (5), and each u_i (i=0,1, ..., L-1) is an output of the nonlinear combiner. Denote the complex weight vector by $\mathbf{W} = [w_0\ w_1 \cdots w_{L-1}]^T$, where w_i, is the weight multiplying u_i. Then, the output of the Volterra equalizer is given by

$$Z = \mathbf{W}^T\mathbf{U} \quad (6)$$

and the weight update equation is given by

$$\mathbf{W}(k+1) = \mathbf{W}(k) + \mu e(k)\mathbf{U}^* \quad (7)$$

where, k is the k-th update time, e(k) is the error at the output of the equalizer at time k, and μ is the step size.

Recall that for a linear adaptive filter (LMS algorithm) convergence is guaranteed only if the step size, μ, is less than

$2/\lambda_{max}$ [7,8], where λ_{max} is the largest eigenvalue of the correlation matrix of the tapped delay line inputs. In addition, when the eigenvalues are widely spread (ratio of $\lambda_{max}/\lambda_{min}$ is large) the rate of convergence is limited by the smallest eigenvalues. Similar conditions hold for the nonlinear equalizer. The following discussion is intended to show that the eigenvalue spread for the nonlinear equalizer is potentially greater than that of the corresponding linear equalizer with N taps.

Consider the correlation matrix of the inputs to the N-tap delay line, for example the correlation matrix of the elements Y_i in figure 2, and denote this matrix as $\mathbf{R}$ and its eigenvalues as λ_i. Define the correlation matrix of the nonlinear combiner outputs, $\mathbf{U}$, as $\tilde{\mathbf{R}}$ and its eigenvalues as α_j. It is clear that $\tilde{\mathbf{R}}$ has dimensions much larger than $\mathbf{R}$ and that the elements of $\mathbf{R}$ are all contained in $\tilde{\mathbf{R}}$. From [8] we have the following two expressions for the maximum and minimum eigenvalues of $\tilde{\mathbf{R}}$

$$\alpha_{max} = \max \frac{x^H \tilde{R} x}{x^H x}, \quad x \in C^L, x \neq 0 \tag{8}$$

and,

$$\alpha_{min} = \min \frac{x^H \tilde{R} x}{x^H x}, \quad x \in C^L, x \neq 0 \tag{9}$$

where L is given by (5) and C^L is complex vector space. Equation (8) states that the largest eigenvalue of $\tilde{\mathbf{R}}$ is obtained by the largest amount by which any vector is amplified by vector multiplication. But since $\mathbf{R} \subset \tilde{\mathbf{R}}$ and $C^N \subset C^L$, then $\alpha_{max} \geq \lambda_{max}$. Similarly, $\alpha_{min} \leq \lambda_{min}$, so that the eigenvalue spread for the nonlinear equalizer is likely to be greater than for the corresponding linear equalizer. Also this implies that the maximum step size is likely to be less for the nonlinear equalizer.

In the next section, the sensitivity to the step size is illustrated with an example. However, before considering such an example, it is useful to investigate a method for improving the convergence characteristics of the nonlinear equalizer. This can be done with the multiple step LMS algorithm [9-12]. With this algorithm each weight may be updated with a unique step size. This leads to the update equation

$$\mathbf{W}(k+1) = \mathbf{W}(k) + \mathbf{M_D} e(k) \mathbf{U}^* \tag{10}$$

where $\mathbf{M_D}$ is a diagonal matrix with the step sizes μ_i (corresponding to weight w_i) along the main diagonal and zeros elsewhere. With the nonlinear equalizer it has been found useful to choose a larger step size for linear terms and smaller step sizes for the nonlinear terms.

If the correlation matrix for the nonlinear combiner output is known then the following illustrates the conditions that must be met to maintain stability. Following a similar approach to [8], it can be shown that the nonlinear equalizer is convergent in the mean (the expectation of the tap weight vector approaches the optimum Wiener solution) and in the mean square, if the largest eigenvalue of the matrix $\mathbf{R_m} = \mathbf{M_D}\tilde{\mathbf{R}}$ is less than 2. Notice that if all the diagonal elements of $\mathbf{R_m}$ are equal then this reduces to the familiar $2/\alpha_{max}$ constraint. As in the linear filtering case, Mueller [12], the update constant may be replaced with $\mu \tilde{\mathbf{R}}^{-1}$ so that all the eigenvalues become unity and all modes decay at the same rate.

IV. Simulation Results

The following results were obtained from Monte-Carlo simulations using a low pass equivalent channel model [3,13]. For the following systems, the M-PSK systems have a square pulse shape at the transmitter and the 16-QAM system has a square root raised cosine with roll-off of one. For all systems the receive filter is matched to the transmit pulse shape. The HPA backoff is defined as the difference, in dB, between the HPA's output saturation power and the average power into the HPA. For the TWT parameters used in this work, the TWT output is saturated with an input power of unity. The M-PSK systems are operated at 0-dB backoff while the 16-QAM systems are operated at various backoffs, as will be indicated for each system. For all the systems considered, the channel pre- and post-filters are 6th-order low-pass butterworth with 3-dB bandwidth of 0.75 R_s.

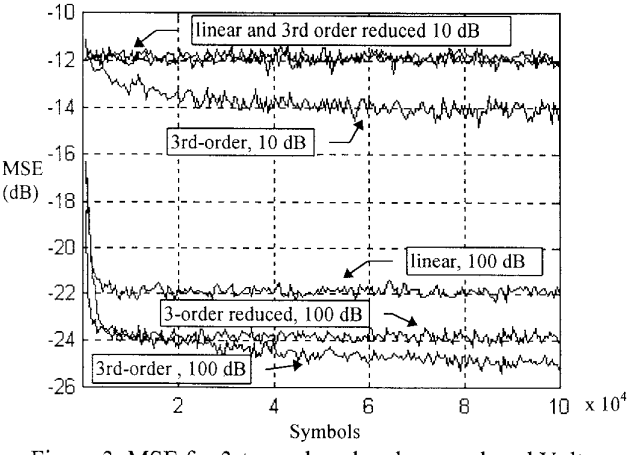

Figure 3. MSE for 3-tap reduced and non-reduced Volterra equalizers at E_b/N_0 = 10 dB, and 100 dB Equalizers.

Fig. 3 plots the mean-square error (MSE) vs. adaption time in symbols for various 3-tap equalizers for a QPSK system. The equalizers are a 3-tap linear equalizer, 3-tap 3rd-order equalizer, and a 3-tap 3rd-order reduced complexity equalizer. The reduced complexity equalizer has the tap weights of the terms $Y_iY_jY_k$ set to zero for i or j = k, as discussed previously. In all cases $\mu = 10^{-3}$. The MSE estimate is obtained by appropriately scaling a 512 symbol running sum of the squared error at the output of the equalizer. This method gives a quick but biased

estimate of the MSE especially before the equalizer has converged. After the equalizer has converged, the method gives a good estimate of the MSE. Although ensemble averaging of learning curves is the proper method for estimating MSE, the computer time necessary for such an approach was prohibitive. The figure illustrates that for low values of E_b/N_0, the reduced equalizer has performance (in MSE) comparable to that of the linear equalizer. As the E_b/N_0 increases the reduced equalizer performance approaches that of the non-reduced equalizer, but still has a performance loss even at very high E_b/N_0. The figure also illustrates that the convergence time for the 3rd-order equalizer is on the order of 100,000 symbols.

Fig. 4 illustrates the advantage of multiple-step size adaption for a QPSK system with an E_b/N_0 of 9 dB. The curve illustrating large jumps and higher overall mean-square error is for a 3-tap 5th-order equalizer with a single step size of 10^{-3}. The lower curve is for a 3-tap 5th-order equalizer with multiple-step adaption and step sizes of 10^{-3}, 10^{-4}, and 10^{-5}, for the linear, 3rd-order, and 5th-order terms, respectively. The single step size equalizer is evidently unstable at this adaption rate. In order to stabilize the single step size equalizer, the step size may be reduced but at the expense of a much slower convergence time. The figure illustrates that the multiple step algorithm lessens the penalty of a slower convergence rate while improving performance in MSE.

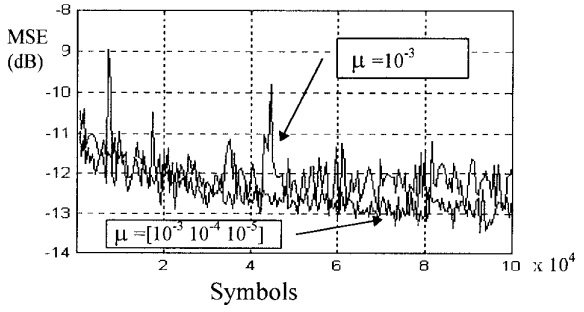

Figure 4. Multiple step size adaption.

The probability of bit error performance for QPSK and 8-PSK systems is shown in Fig. 5. For the QPSK system the equalizers are a 5-tap linear and 5-tap 3rd order. For the 8-PSK system the equalizers are a 7-tap linear, 7-tap 3rd-order, and 7-tap linear with 3-tap 3rd-order. The latter equalizer utilizes only the 3 center taps for nonlinear equalization. Although, according to Fig. 3, the MSE performance for a 3rd-order equalizer is approximately 2 dB better than for a linear device, there is no improvement in P_b for QPSK.

Some insight may be obtained by looking at a scatter plot of the equalizer output, Fig. 6. For this case it has been determined that the signal to distortion ratio is approximately 15 dB whereas the symbol energy to noise spectral density ratio is 13 dB (i.e. E_b/N_0 = 10 dB). With the distortion below or at a comparable level to the noise, the equalizer can significantly reduce the mean-square error by reducing the component of the noise in the radial direction, however, this noise reduction

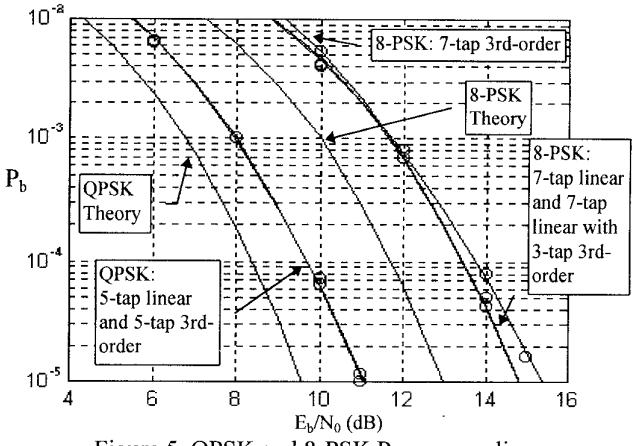

Figure 5. QPSK and 8-PSK P_b error nonlinear equalizer performance.

is orthogonal to the direction which leads to a decision error. Thus, although the mean-square error is significantly reduced, the probability of error is not improved. This result is unique to M-PSK when the distortion is below the noise level. In the 8-PSK case, the noise level is below the distortion at $P_b = 10^{-5}$ and the 3rd-order nonlinear equalizers give a 0.5 dB improvement in P_b.

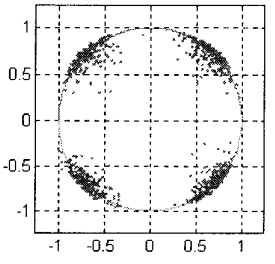

Figure 6. Scatter plot: 5-tap 3rd-order equalizer output.

The 7-tap 3rd-order equalizer (343 3rd-order terms) shows a slightly degraded performance compared to the linear equalizer at low E_b/N_0 due to noise enhancement. The 7-tap linear 3-tap 3rd-order equalizer (7 linear terms, 27 3rd-order terms) gives the same performance improvement at high E_b/N_0 at a much lower complexity compared to the former.

Thus far only constant modulus systems have been considered. Figure 7 illustrates the performance in P_b for a 16-QAM system. Several equalizer configurations are considered: 9-tap linear, 9-tap 3rd-order, and 9-tap linear with 3-tap 3rd-order. For the linear equalizer, the 16-QAM system must be operated a large backoff for low P_b. However the 3rd-order nonlinear equalizers can operate at 6-dB backoff and still maintain a low P_b. The 9-tap 3rd-order (9 linear and 729 3rd-order terms) has approximately 0.5 dB better performance than the 9-tap linear 3-tap 3rd-order equalizer (9 linear, and 27 3rd-order terms) however the former is an impractical device. The significant improvement for the nonlinear equalizers is in link margin. The 9-tap linear 3-tap 3rd-order equalizer at 6 dB

backoff gives approximately a 4 dB improvement in link margin compared to the 9-tap linear device at 10 dB backoff.

The nonlinear equalizer improvement in P_b for 16-QAM versus PSK systems is attributed to two dominate factors: 16-QAM operates at a higher E_b/N_0 than the PSK systems and QAM is subject to constellation warping [6] so that the effects of the HPA are more significant. In contrast to constellation warping, PSK suffers a constellation rotation which is reversed by the phase synchronizer. Note also that the link penalty for the PSK systems considered is not nearly as severe compared to the QAM system.

V. Conclusions

The Volterra equalizer was extended to an adaptive equalizer utilizing the LMS and multiple step LMS algorithms. Although the nonlinear equalizers gave significant improvement in MSE, no improvement in P_b was found for a QPSK system where the noise level was greater than signal distortion. A modest improvement in probability of error for an 8-PSK system was demonstrated and it is expected that a greater improvement exists for 16-PSK where the distortion level is greater than the noise level. For 16-QAM modulation the nonlinear equalizers gave a significant improvement in link margin. The complexity of the equalizers was discussed and it was that shown that simplified nonlinear devices (i.e. N-tap linear with 3-tap 3rd-order) give performance improvement comparable to extremely complex (i.e. N-tap linear, N-tap 3rd-order) non-simplified devices.

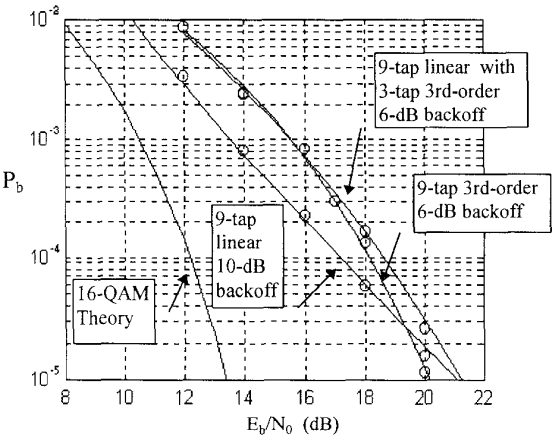

Figure 7. 16-QAM P_b performance for nonlinear equalizers.

References

[1] D. D. Falconer, "Adaptive equalization of channel nonlinearities in QAM data transmission," *Bell Syst. Tech. J.,* vol. 57, no. 7, pp. 2589-2611, Sept. 1978.

[2] S. Benedetto and E. Biglieri, "Nonlinear equalization of digital satellite channels, "*IEEE J. Select. Areas Commun.,* vol. SAC-1, pp. 57-62.

[3] S. Benedetto, E. Biglieri, and R. Daffara, "Modeling and performance evaluation of nonlinear satellite links - A Volterra series approach," *IEEE Trans. Aerosp. Electron. Syst.,* vol. AES-15, pp. 494-507, July 1979.

[4] G. Karam and H. Sari, "Analysis of predistortion, equalization, and ISI cancellation techniques in digital radio systems with nonlinear transmit amplifiers," *IEEE Trans. Commun.,* vol. 37, pp. 1245-1253, Dec. 1989.

[5] A. A. M. Saleh, "Frequency-independent and frequency-dependent nonlinear models of TWT amplifiers, " *IEEE Trans. Commun., vol.* COM-29, pp. 1715-1720, Nov. 1981.

[6] S. Pupolin and L. J. Greenstein, "Performance analysis of digital radio links with nonlinear transmit amplifiers, " *IEEE J. Select. Areas Commun.,* vol. SAC-5, pp. 534-546, Apr. 1987.

[7] B. Widrow and S.D. Stearns, *Adaptive Signal Processing.* Englewood Cliffs, NJ: Prentice-Hall, 1985.

[8] S. Haykin, *Adaptive Filter Theory.* Englewood Cliffs, NJ: Prentice-Hall, second edition, 1991.

[9] C. S. Modlin and J. M. Cioffi, "A fast Decision Feedback LMS Algorithm Using Multiple Step Sizes," in *Proc IEEE Int'l Conf. on Comm.*,pp. 1201-1205, May 1993.

[10] R. W. Harris, D. M. Chabries, and F. A. bishop. "Avariable step (VS) adaptive algorithm." *IEEE Transactions on Acoustics, Speech, and Signal Processing,* pp. 309-316, April 1986.

[11] W. B. Mikhael, F. H. Wu, L.G. Kazovsky, G. S. Kang, and L. J. Fransen. "Adaptive filters with individual adaption of parameters." *IEEE Transactions on Circuits and Systems,* vol. CAS-33, pp. 677-686, July 1986.

[12] K. H. Mueller. "A new, fast converging MS algorithm for adaptive equalizers with partial response signaling" , *Bell Syst. Tech. J.,* Jan. 1975

[13] M.C. Jeruchim, P. Balaban, and K.S. Shanmugan, *Simulation of Communication Systems,* Plenum Press, New York, NY, 1992.